Waters, M. G., & Blobel, G. (1986) *J. Cell Biol. 102*, 1543-1550.
Watts, C., Silver, P., & Wickner, W. (1981) *Cell (Cambridge, Mass.) 25*, 347-353.
Watts, C., Wickner, W., & Zimmermann, R. (1983) *Proc. Natl. Acad. Sci. U.S.A. 80*, 2809-2813.
Wickner, W. (1975) *Proc. Natl. Acad. Sci. U.S.A. 72*, 4749-4753.
Wickner, W. (1979) *Annu. Rev. Biochem. 48*, 23-45.
Wickner, W., & Lodish, H. (1985) *Science (Washington, D.C.) 230*, 400-407.
Wiech, H., Sagstetter, M., Muller, G., & Zimmermann, R. (1987) *EMBO J. 6*, 1011-1016.
Wolfe, P. B., Silver, P., & Wickner, W. (1982) *J. Biol. Chem. 257*, 7898-7902.
Wolfe, P. B., Wickner, W., & Goodman, J. M. (1983) *J. Biol. Chem. 258*, 12073-12080.
Wolfe, P. B., Rice, M., & Wickner, W. (1985) *J. Biol. Chem. 260*, 1836-1841.
Zimmermann, R., & Wickner, W. (1983) *J. Biol. Chem. 258*, 3920-3925.
Zimmermann, R., & Meyer, D. I. (1986) *Trends Biochem. Sci. (Pers. Ed.) 11*, 512-515.
Zimmermann, R., & Mollay, C. (1986) *J. Biol. Chem. 261*, 12889-12895.
Zimmermann, R., Watts, C., & Wickner, W. (1982) *J. Biol. Chem. 257*, 6529-6536.
Zwizinski, C., & Wickner, W. (1980) *J. Biol. Chem. 255*, 7973-7977.
Zwizinski, C., & Wickner, W. (1982) *EMBO J. 1*, 573-578.

Articles

A Description of Conformational Transitions in the Pribnow Box of the trp Promoter of *Escherichia coli*†

Jean-François Lefèvre,‡ Andrew N. Lane,§ and Oleg Jardetzky*
Stanford Magnetic Resonance Laboratory, Stanford University, Stanford, California 94305
Received March 31, 1987; Revised Manuscript Received July 21, 1987

ABSTRACT: Selective changes in the NMR parameters of the sequence of CGTACTAGTTAACTAGTACG, which corresponds to the trp operator of *Escherichia coli*, were observed as a function of temperature. The changes were localized to the sequence TTAA in the Pribnow box (underlined). Differential changes in chemical shift were analyzed in terms of a three-state model (states I, II, and III) to give the equilibrium constants, enthalpy changes, and populations. The midpoints of the first and second transitions were 9 and 30 °C, with enthalpy changes of 58 and 35 kcal/mol, respectively. Measurement of the spin-lattice and cross-relaxation rate constants at different temperatures allowed some structural conclusions to be drawn about the nature of the transitions. The line width of the H2 of A11 goes through a maximum at about 30 °C, indicating moderately fast exchange between the states. The rate constants for exchange at the midpoints were about 200 (I ↔ II) and 250 (II ↔ III) s^{-1}. Taking these findings into account, we propose a mechanism for the interaction between RNA polymerase and the promoter. This mechanism can explain the temperature dependence observed for the initiation of transcription.

The initiation of transcription by prokaryotic RNA polymerase is for many purposes adequately described by the two-step reaction scheme (Chamberlin, 1974) depicted in Scheme I, where R is RNA polymerase, P is the promoter, RPc is the initial "closed" complex which is thought to involve recognition of a sequence [consensus TTGACA (Rosenberg & Court, 1979; Hawley & McClure, 1983)] found near the −35 region, and RPo is the active "open" complex (Siebenlist, 1979) from which transcription occurs. It is generally thought that the isomerization of RPc to RPo occurs in the Pribnow box [consensus sequence TATAAT (Rosenberg & Court, 1979; Hawley & McClure, 1983)] located at −10. The rate constant of this process is relatively small, ranging from 0.01 to 1 s^{-1}, depending on the strength of the promoter. The formation of the open complex may involve a number of mechanisms which have not yet been fully elucidated but is probably a multistep process (Bertrand-Burgraff et al., 1984; Buc & McClure, 1985). The formation of the open complex is strongly dependent on the temperature, having an apparent midpoint in the range 15–25 °C, depending on the promoter (Chamberlin, 1974; Richardson, 1975; Dausse et al., 1976; Suzucki et al., 1976). Studies of the temperature dependence of the formation of the open complex have led to the conclusion that an intermediate state becomes significantly populated at low temperatures. This additional state should be inserted between RPc and RPo in Scheme I (Kadesh et al., 1981; Roe et al., 1984; Buc & McClure, 1985).

Scheme I

$$R + P \leftrightarrow RPc \leftrightarrow RPo \rightarrow \text{transcription}$$

We have been studying the structure and solution properties of the trp operator/promoter (sequence CGTACTAGTTAACTAGTACG) by NMR[1] (Lefèvre et al., 1985a,b;

† This work was supported by NIH Grants RR00711 and GM33385. J.-F.L. gratefully acknowledges a fellowship from La Fondation pour la Recherche Médicale.
‡ Present address: Institut de Biologie Moléculaire et Cellulaire, 15 Rue Descartes, 6700 Strasbourg, France.
§ Present address: National Institute for Medical Research, The Ridgeway, Mill Hill, London NW7 1AA, U.K.

0006-2960/88/0427-1086$01.50/0

Lane et al., 1986a–c). We have assigned all of the imino protons and have measured their rates of exchange as a function of temperature and pH (Lefèvre et al., 1985a). We have also assigned most of the nonexchangeable protons and have determined the structure in solution using a combination of relaxation times, coupling constants, and nuclear Overhauser enhancements with the aid of a new method of data analysis (Lefèvre et al., 1987). While systematically investigating the conformation of the DNA as a function of temperature, we noted changes in NMR parameters specific to the sequence TTAA in the Pribnow box region (underlined in the above sequence), which we interpreted as a localized conformational change (Lefèvre et al., 1985b). Important effects on the rate of transcription related to the presence of the sequence TTAA have been noted in other systems such as in the CAAT box of the gene for Ag globin (Collins et al., 1985; Gelinas et al., 1985). It is important, therefore, to characterize as fully as possible the conformational features of the sequence TTAA.

In this paper we analyze in detail the changes in conformation of the Pribnow box that occur as the temperature is varied. On the basis of these results, we propose a new reaction scheme for the initiation of transcription, which incorporates the conformational changes in the Pribnow box and accounts for the observed temperature dependence of the initiation of transcription.

Materials and Methods

Trp operator DNA (CGTACTAGTTAACTAGTACG) which also contains the Pribnow box (underlined) of the trp promoter was purchased from P-L Biochemicals Ltd. and used without further purification. The oligonucleotide was annealed as previously described (Lefèvre et al., 1985a). The final concentration was 1.4 mM duplex (2.8 mM strands) in 100% D_2O containing 10 mM sodium phosphate buffer and 100 mM NaCl, pD* 8.5, where pD* is the uncorrected pH meter reading.

Proton NMR spectra were recorded on a JEOL GX 500 spectrometer and referenced to internal 2,2′-dimethylsilapentane-5-sulfonate (DSS). For accurate determination of chemical shifts, the spectra were enhanced in resolution by multiplying the free induction decays (FID) with a positive exponential (4-Hz line broadening) and a trapezoid function (0, 15, 30, and 95% of the FID).

Spin–spin relaxation times (T_2) were obtained with the Carr–Purcell–Meiboom–Gill sequence. Selective spin–lattice relaxation times (T_1) were measured by saturation recovery as previously described (Lefèvre et al., 1985a) with a saturation pulse of 25 ms. Relaxation data were analyzed by nonlinear regression to the appropriate equations.

Driven, truncated nuclear Overhauser enhancements (NOEs) were measured according to Wagner and Wüthrich (1979) in the high-power limit (Bothner-By & Noggle, 1979). For NOEs between sugar and base protons, one time point was recorded at each temperature. For NOEs between H2's of neighboring adenine residues, three or four time points were recorded, and the cross-relaxation rate was estimated from the initial slope of the plot of NOE versus irradiation time.

Thermodynamic parameters were estimated from temperature-dependent studies by an interactive gradient search algorithm. Structural parameters were determined from nuclear Overhauser enhancements according to the method described (Lefèvre et al., 1987).

[1] Abbreviations: NMR, nuclear magnetic resonance; NOE, nuclear Overhauser effect; FID, free induction decay.

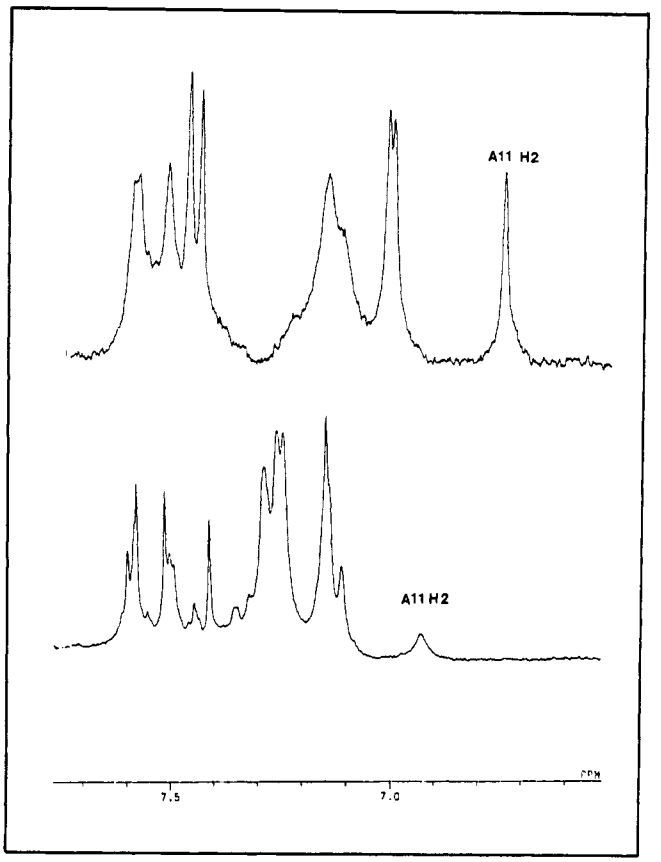

FIGURE 1: Effect of temperature on the NMR spectrum of the trp operator-promoter. NMR spectra were recorded at 500 MHz in 100% D_2O. The H6/H2 region is shown. The spectra have 2-Hz line broadening added. Upper spectrum; 0 °C; lower spectrum; 25 °C.

Errors were estimated from the inverse of the curvature matrix (Bevington, 1969) and the variance of the data.

Results and Discussion

We have determined several structural parameters of the trp operator at 25 °C (Lefèvre et al., 1987) and have shown that there are sequence-dependent variations in agreement with the predictions of the rules of Calladine (1982) and Dickerson (1983). We also argued on the basis of the temperature dependence of the intrinsic spin–lattice relaxation rate constants that the structure of the Pribnow box region changes as the temperature is raised. We have previously reported that there are temperature-dependent transitions detectable by NMR in the trp operator (Lefèvre et al., 1985b). Conformational states are expected to differ in enthalpy, and therefore, the populations of different states should be temperature dependent. Here we give a detailed analysis of the thermodynamics and structural changes associated with the conformational transitions.

Figure 1 shows NMR spectra of the H6/H2 region of the trp operator at 0 and 25 °C. The spectra are markedly different. The most striking feature is the width of the H2 resonance of A11, which is much broader at 25 than at 0 °C, in contrast to the other resonances which become sharper as the temperature is raised. This suggests that the region around A11, which is in the Pribnow box, undergoes a temperature-dependent conformational change in this temperature range. In fact, over the range 0–45 °C there are selective changes in the NMR parameters (chemical shifts, spin–lattice relaxation rate constants, line widths, and cross-relaxation rate constants) of protons of the bases in the Pribnow box only, and not in other regions of the operator-promoter.

We have measured the chemical shifts, line widths, intrinsic spin–lattice relaxation times, and a number of cross-relaxation rate constants as a function of temperature. These parameters are all sensitive to conformation. As changes in some of these parameters are not monotonic, it is necessary to invoke a multistep model to account for the observed conformational changes. We will demonstrate that the selective changes in chemical shifts allow the population of each state as a function of temperature to be determined. In addition, the changes in relaxation rate constants allow the conformational changes to be interpreted in structural terms. The conformational changes are restricted to an important control region, the Pribnow box.

Selective Changes in Chemical Shifts Are Observed as a Function of Temperature. It is generally observed that the chemical shifts of base protons in B DNA, which are dominated by ring currents of neighboring bases (Arter & Schmidt, 1976), change monotonically with temperature. This can be attributed to the change in the bulk magnetic susceptibility (Jardetzky & Roberts, 1981) and to a general and continuous change in helical twist. In the absence of so-called premelting transitions (Patel et al., 1982, 1985b), the variation of chemical shift with temperature is linear below the melting transition and characterizes each kind of proton. In the trp operator, the chemical shifts of the H8's of A4, A7, A15, and A18 decrease linearly as the temperature is increased, with a common slope of −1.4 ppb/deg. The H8's of the guanosine residues behave similarly. The chemical shifts of the H2's of A4, A7, A15, and A18 change in parallel, but with a slope of +1.4 ppb/deg (data not shown).

However, the chemical shifts of the H2 and H8 of the central adenosines, A11 and A12, behave very differently. The dependence of the chemical shifts of these protons on temperature was reported previously (Lefèvre et al., 1985b). The observed chemical shifts can be corrected for the intrinsic dependence on temperature below the global melting temperature (55 °C under the conditions of these experiments) as previously described (Lefèvre et al., 1985b). The excess chemical shifts of the H2 resonances of A11 and A12 are strongly sensitive to the temperature and vary approximately linearly over the range 0–45 °C (slope = 0.94 Hz/deg for A11 H2 and −0.63 Hz/deg for A12 H2; note the opposite sense of the change of these neighboring protons). However, the excess chemical shift of A11 H8 passes through a maximum, whereas that of A12 follows normal behavior. As the chemical shift is sensitive to the conformation, these selective changes reveal structural or dynamic features of the central region of the trp operator, which also corresponds to the Pribnow box of the trp promoter.

Chemical Shifts Can Be Analyzed According to a Three-State Model. Given the nonmonotonic behavior of the chemical shift of the H8 of A11, it is not possible to fit the data using only two states; at least three states must become significantly populated over this range of temperatures. The simplest model is therefore one involving three states, which we denote as states I, II, and III:

$$\mathrm{I} \overset{K_1}{\leftrightarrow} \mathrm{II} \overset{K_2}{\leftrightarrow} \mathrm{III} \qquad (1)$$

where K_1 and K_2 are equilibrium constants. This represents the minimal scheme required for describing the behavior of the different parameters with temperature. Other multistate models may also account for the data. The data do not permit a choice between different multistate models, because they represent time averages (Jardetzky, 1980). The three-state model developed below is the simplest phenomenological description of our observations.

Table I: Thermodynamics of the Transitions in the Pribnow Box[a]

parameter	transition I → II	transition II → III
ΔH_i (kcal/mol)	58 ± 3.4	34 ± 1.9
K_i (0 °C)	0.023 ± 0.004	0.0024 ± 0.0005
t_m (°C)	10 ± 2	30 ± 3
$\Delta\delta$ A11 H8 (Hz)	10.7 ± 0.4	−10 ± 0.4
$\Delta\delta$ A11 H2 (Hz)	19 ± 4	41 ± 3
$\Delta\delta$ A12 H2 (Hz)	−10 ± 2	−21 ± 3
k_i at t_m (s^{-1})	200 ± 40	250 ± 50

[a] The reference state is 0 °C, as described in the text. ΔH_i are the enthalpy changes of the two transitions, K_i are the equilibrium constants at 0 °C, t_m at the temperatures at which $K_i = 1$, and $\Delta\delta$ are the chemical shift differences between the states, corrected for the intrinsic dependence on temperature as described in the text. k_i are the rate constants for the transitions between the states at the midpoint temperature.

Because the chemical shift changes continuously with increasing temperature (cf. Figure 1), rapid exchange conditions hold. The observed chemical shift is then the weighted sum of the intrinsic chemical shifts of states I, II, and III (Sandström, 1982), i.e.

$$d(T) = \sum X_i(T) d_i \qquad (2)$$

with $i = 1$–3, where $X_i(T)$ are the mole fractions at temperature T. The temperature dependence of the corrected chemical shift is then due to the dependence of the fractional populations, X_i, on temperature. The fractional populations can be related to the equilibrium constants by

$$X_1 = 1/(1 + K_1 + K_1K_2) \qquad (3a)$$

$$X_2 = K_1X_1 \qquad (3b)$$

$$X_3 = 1 - X_1 - X_2 \qquad (3c)$$

The two equilibrium constants are related to the enthalpy changes ΔH_i according to

$$K_i(T) = K_i(T_0) \exp[-(\Delta H_i/R)(1/T - 1/T_0)] \qquad (4)$$

where T_0 is a reference temperature, in this case 273 K, and R is the gas constant. We have fitted the excess chemical shift of A11 H8 to eq 2–4. The best fit parameters are given in Table I. In order to reduce the number of free parameters to be fitted, we took the chemical shift difference of state III − state I to be zero (Lefèvre et al., 1985b). Owing to the exponential dependence of the chemical shift on the enthalpy changes, these parameters are well determined (estimated error ≈ ±6%). The equilibrium constants at 0 °C are less well determined (estimated error ≈ ±20%). There is also significant covariance between some of the parameters. The largest covariances are between the two enthalpy differences, and the maximum chemical shift difference is with the two enthalpy changes. Thus, a fit within the variance of the data can be obtained by increasing or decreasing the enthalpies together or by increasing the the maximal chemical shift difference and decreasing both enthalpy changes. The other parameters are essentially independent.

The quality of the fit is shown by the drawn curve in Figure 2A. The shaded area represents the degree of uncertainty associated with the variances of the best fit parameters. This justifies our assumption of a three-state model: although more states cannot be ruled out, they are not warranted by the data.

Having calculated the enthalpy changes and equilibrium constants, it is possible to calculate the populations at each temperature, with eq 3. The populations are shown in Figure 2B. Again, the dotted lines represent the error in the popu-

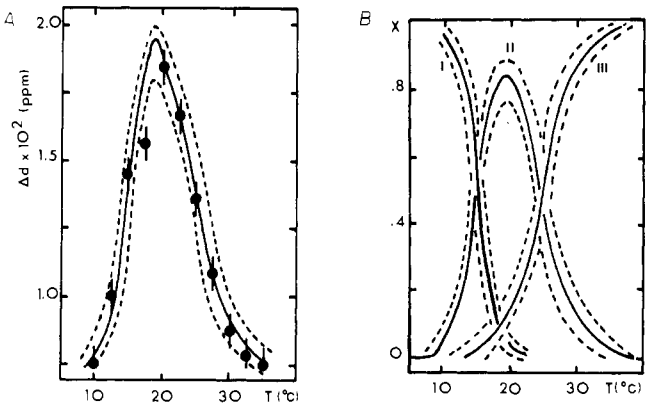

FIGURE 2: Dependence of the chemical shift of A11 H8 on temperature. (A) The chemical shift was corrected as described in the text and in Lefèvre et al. (1985b). The continuous line is the best fit line with the parameters given in Table I, and the dotted lines show the range according to the variance of the parameters in Table I. (B) Populations of states I, II, and III as a function of temperature were calculated with eq 3 as described in the text. The dotted lines show the error associated with the variance of the parameters in Table I.

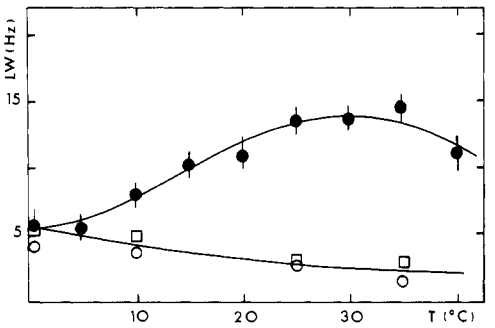

FIGURE 3: Dependence of line widths of H2 resonances on temperature. Line widths were estimated as the width at half-height, minus the line broadening (1 Hz). (●) A11 H2; (□) A4 H2; (○) A12 H2. The line drawn through the points for A12 and A4 is for the dependence of the relaxation rate on viscosity according to $LW(T) = LW(0)\eta(T)T_0/\eta(T_0)T$, where LW(0) is the line width at 0 °C, $\eta(T,T_0)$ is the viscosity of D_2O at temperature T and 0 °C, and T is the absolute temperature. The line through the points of A11 was drawn by eye.

lations associated with the variance of the parameters in Table I. The midpoint temperature (t_m) at which $K_i = 1.0$ can be calculated. These are also given in Table I. Interestingly, the three states are well separated on the temperature scale, with midpoint temperatures of 10 ± 2 and 30 ± 3 °C for the two transitions, respectively. This is fortunate, as the conformations of the three states can be obtained by performing measurements at the appropriate temperatures.

Finally, the variations of the chemical shifts of A11 H2 and A12 H2 as a function of temperature can be fitted by use of the calculated population differences, yielding the chemical shift changes for the two transitions. These are also given in Table I.

Changes in Line Widths Indicate That the Transitions Are in Intermediate Exchange on the Chemical Shift Time Scale for the H2 of A11. The dependence of line widths of A H2's on temperature is shown in Figure 3. At 0 °C, where only state I is significantly populated (see Figure 2B), all the line widths are similar and also agree with independent estimates of the spin–spin relaxation time. These resonances are generally observed to be sharp because in a B-type double helix the protons are relatively distant from their nearest neighbors (Kearns, 1984). The line widths of the H2's of A4, A12, and A18 decrease monotonically in the range 0–45 °C and, in fact, follow the expected viscosity law for a rigid body. On the other hand, the line width of the H2 of A11 goes through a maximum at about 30 °C, showing an excess line width of about 11 Hz at this temperature.

The simplest explanation of this result is that the rates of exchange among the three conformations are comparable to the chemical shift differences (Sandström, 1982). Further, the observed chemical shift changes progressively (cf. Figure 2A), indicating moderately fast exchange. The alternative explanation, that other protons approach the H2 of A11, would require impossible changes in conformation to account for the observed increase in line width. According to relaxation data (see below), this could not account for more than about 0.5 Hz in the line width.

At the midpoint temperatures, 10 and 30 °C, the forward and reverse rate constants are equal. Given the chemical shift differences between states I and II and between states II and III (cf. Table I), it is possible to estimate the rate constants at the midpoint temperatures (Sandström, 1982). The values are about 200 s^{-1} for the first transition and 250 s^{-1} for the second transition. Spectral simulations including the effects of chemical exchange on the line widths and resonance frequency (data not shown) also support these values for the rate constants. The activation energy for the forward rate constants must be at least equal to ΔH_i, which implies that the rate constants are highly temperature dependent. It was therefore not possible to obtain accurate values of the rate constants over the whole temperature range given the experimental errors and relatively sparse data set.

As the chemical shift differences for the H8's are ≈10 Hz, the transitions are in the rapid exchange limit, so that no differential line broadening is observed for these protons. This also justifies our analysis of the changes in chemical shifts of the H8's, on the assumption of rapid exchange.

Changes in Spin–Lattice Relaxation Rate Constants Can Also Be Accounted for by the Three-State Model. The conformational transitions can also be monitored by measuring the intrinsic spin–lattice relaxation rate constant (r_1) as a function of temperature. The variation of r_1 was corrected for the viscosity effect and normalized to 0 °C as follows:

$$\rho_1^{cor} = \rho_1^0(273)\eta(T)/T\eta(0) \qquad (5)$$

where ρ_1^0 is the relaxation rate constant at 0 °C, T is the absolute temperature, and η is the viscosity. The temperature dependence of the viscosity of ^2H_2O was estimated from the data of Wilbur et al. (1976). The corrected ρ_1 values for A4, A7/15, A18, A11, and A12 are shown in Figure 4. For A4, A7/15, and A18, the value of ρ_1^{cor} is independent of the temperature, showing that these protons are not affected by the conformational transitions. This is consistent with the apparent activation energy calculated from the temperature dependence of the spin–lattice relaxation rates of these protons (≈4 kcal/mol; Lefèvre et al., 1987). On the other hand, both the H8 and the H2 of A11 deviate considerably from the horizontal line observed for the other bases, such that the ρ_1 values show a weaker dependence on temperature than expected from changes in viscosity. Indeed, for the H2 of A11, the corrected ρ_1 goes through a maximum, again indicating that a three-state model is the minimum necessary to describe the data. With the populations calculated above, the ρ_1 values for each state can be calculated. At 0 °C, the spin–lattice relaxation rate constant, ρ_1, for A11 H2 is 2.1 s^{-1} in state I, 7.5 s^{-1} in state II, and 4.6 s^{-1} in state III. The curve in Figure 4B represents the fit to the three-state model, with the populations calculated from the chemical shift data (Figure 2B). Again, the three-state model gives an adequate description of the data. Similar calculations yield the values of ρ_1 at 0 °C

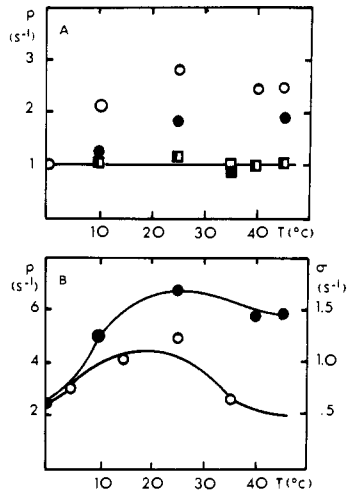

FIGURE 4: Dependence of the spin–lattice and cross-relaxation rate constants on temperature. Spin–lattice and cross-relaxation rate constants were determined as described under Materials and Methods. Relaxation rate constants were corrected for differences in viscosity. (A) Temperature dependence of spin–lattice relaxation rate constants. These were also normalized to the value at 0 °C: (●) A11 H2, (○) A11 H8, (■) A4, A7/15, and A18 H2, and (□) A4, A7/15, and A18 H8. (B) A11 H2 (●) spin–lattice relaxation rate constant (right-hand scale) and (○) cross-relaxation rate constant (left-hand scale) between A11 and A12 H2's fitted to the three-state model, as described in the text.

Table II: Intrinsic Spin–Lattice Relaxation Rate Constants of H8 and H2 Resonances of A11 and A12[a]

	ρ_1 (s^{-1})		
proton	I	II	III
A11 H8	8.8	14.6	12.9
A11 H2	2.1	7.5	4.6
A12 H8	11.3	16	9.0
A12 H2	3.9	4.3	3.4

[a] The relaxation rate constants at 0 °C in states I, II, and III were determined from the values observed at different temperatures and the populations given in Figure 2B.

for A11 H8 and A12 H8 and H2. These values are given in Table II.

Structure and Possible Structural Changes of the Central Region at 25 °C. We have determined the structure of the whole trp operator at 25 °C, which corresponds to state II (Lefèvre et al., 1987). We have measured cross-relaxation rate constants between the base and sugar protons in the Pribnow box at 0 and 40 °C to determine the changes in structure in the transitions II to I and II to III, using the structure determined at 25 °C as a reference.

(a) Changes in Distance between the A11 and the A12 H2's. For sequences containing successive AT pairs, the cross-relaxation rate constants between H2's in the minor groove can also be used to determine changes in propellar twists (Patel et al., 1983). We have measured the cross-relaxation rate constant for A11 H2 to A12 H2 as a function of temperature (Lefèvre et al., 1985b). The dependence of the cross-relaxation rate on temperature, corrected for the effect of viscosity, is shown in Figure 4B. With the fractional populations (Figure 2B), the cross-relaxation rate constants in each state were calculated according to eq 2, with δ replaced by σ. The cross-relaxation rates are given in Table III. The distance between the H2's can be estimated from the cross-relaxation rate constants, provided that there are no alternative pathways of magnetization transfer (Lefèvre et al., 1987), according to

$$\sigma = -\alpha\tau_c/10r^6 \qquad (6)$$

Table III: Apparent Cross-Relaxation Rate Constants in the Pribnow Box[a]

		σ (s^{-1})		
base	NOE	state I	state II	state III
T9	intra H2″ → H6	−1.7	−1.6	−1.5
	intra H1′ → H6	−0.8	−0.8	−0.6
T10	intra H6 → H1′	−1.0	−0.8	−1.4
	inter H1′(T9) → H6	−1.3	−0.8	−0.7
A11	intra H2″ → H8	−1.5	−1.0	−0.6
	intra H1′ → H8	−0.4	−0.2	−0.5
	inter H2″(T10) → H8	−2.3	−0.7	−1.0
A12	H2″(A12 + A11) → H8	−2.1	−1.4	−0.9
	inter H1′(A11) → H8	−0.2	−0.2	−0.5
C13	inter H2″(A12) → H8	−0.7	−1.3	−0.5
A11/A12	inter H2 → H2	−0.7	−1.3	−0.5

[a] The cross-relaxation rate constants were determined as described in the text and are normalized to 25 °C. For NOEs between base and sugar protons, the apparent s is defined as NOE/t, where t = 200 ms for H1′–H8/6 and t = 100 ms for other pairs of protons. The cross-relaxation rate constants for A11 H2–A12 H2 are taken from the initial slope of the NOE buildup curve. The values are in s^{-1}. The probable error on NOEs is about ±20%.

where $\alpha = 5.692 \times 10^{-37}$ cm^6 s^{-2}, τ_c is the rotational correlation time, and r is the internuclear distance. We have estimated the correlation time as 6.4 ns at 298 K (Lane et al., 1986a–c). Hence, the internuclear distance in state I is 3.2 Å, decreasing to 3.0 Å in state II and increasing again to 3.4 Å in state III.

The distance in state II can be independently estimated from the structural parameters given in Table III. This gives 3.5 Å at 25 °C. This discrepancy can be accounted for partly by imprecision in the data and partly by internal motion. Internal motion has two effects on the observed cross-relaxation rate constant. The first is that the correlation time is decreased, thereby decreasing the apparent distance. However, calculations show that reasonable internal motions have only a small effect on the correlation time. Further, we have shown that internal motions of AT base pairs in the trp operator are insignificant on the nanosecond time scale (Lane et al., 1986a–c). The second effect is that the internuclear distance changes during the motion, so that the distance of closest approach is more heavily weighted (cf. eq 6). Motions that affect the distance are helical twisting and propeller twisting. Calculations show that changes of the twist angle between A11 and A12 of 20° and changes of the propeller twist of about 20° can change the apparent distance from 3.5 to 3.0 Å. This underlines the difficulty in determining structures from distance measurements, as only averages are in fact observed. However, we are more concerned with changes in distances than with their absolute values, as they provide information on the amplitudes of the structural changes. We note also that the apparent A H2–A H2 distances obtained according to a similar method by Patel et al. (1983) in the sequence CGCGAATTCGCG are significantly shorter than those estimated from X-ray fiber diffraction, but the sign and size of the propeller twists were reasonably well reproduced.

Changes in the base pair twist angle, in the roll angle of each base, or in the pitch can account for the variation of the distance between A11 H2 and A12 H2 in the three states. The magnitude of the effect on the distance is essentially linear in the above parameters for small displacements from the mean values characterizing state II. Thus, the distance changes 0.04 Å/deg for the roll angle of A12, −0.04 Å/deg for the roll of A11, and 0.023 Å/deg for the twist angle. An increase in the pitch yields 0.82 Å/Å. Hence, a change of 0.5 Å for state II to state I could result from a change of the roll angle of 10°, a change of 20° in the helical twist, or a change of 0.5 Å in the pitch. Given the structural constraints of the neighboring

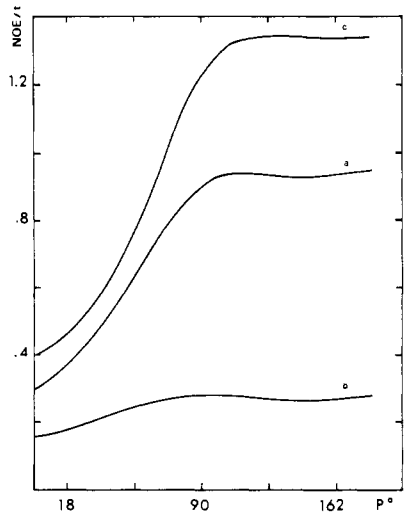

FIGURE 5: Simulation of the apparent cross-relaxation rate constant as a function of the sugar pucker for A11. The structural parameters used were those corresponding to state II (see Table III) and except for the pseudorotqation phase P were kept constant. (a) Intra H2″–H8 of A11, σ_{app} at 100 ms; (b) intra H1′–H8 of A11, σ_{app} at 200 ms; (c) A11 H2″–A12 H8, σ_{app} at 200 ms.

base pairs, the latter two are extremely unlikely. More reasonable is that the change in distance reflects a combination of two or more of these parameters.

(*b*) *Structural Changes of the Nucleotide Units and of Their Respective Orientation.* The structures of the nucleotide units can be adequately described by two parameters, the pucker pseudorotation phase angle P and the glycosidic torsion angle X. These parameters can be reliably estimated from the cross-relaxation rate constants, H1′ and H2′ to the H8 or H6. The relative orientations of successive nucleotide units can be determined from internucleotide NOEs, such as H2″ and H1′ to the H8 or H6 (Lane et al., 1986a–c; Lefèvre et al., 1987). We have measured these cross-relaxation rate constants as a function of temperature. The characteristic values of each state were then calculated as described above and are given in Table III, normalized at 25 °C. Some values are changing as a function of temperature, indicating that the nucleotide conformations are changing.

From the results in Table III, it is clear that the structure of T9 does not alter in either transition nor does that of T10 during the transition from state I to state II. However, the NOE from H1′ to H6 (intra) of T10 increases from state II to state III, suggesting that the glycosidic torsion angle changes.

On the other hand, the structure of A11 changes in both transitions, as does its orientation with respect to T10. The change in the structure of A11 is mainly a change in the sugar pucker. Figure 5 shows a simulation of these NOEs as a function of the deoxyribose conformation, using a fixed value of the glycosidic torsion angle corresponding to that found at 25 °C. Between P = 90° and P = 180°, the NOEs are insensitive to the pucker. At 25 °C (i.e., state II), the value of P is 126°. Going to low temperature, i.e., toward state I, the H2″–H8 NOE increases, requiring that the glycosidic torsion angle decreases. In the transition to state II, the same NOE decreases, consistent with a decrease in the value of P (i.e., toward C2′-endo). Variation of the H1′–H8 NOE, shown in Figure 6, would not be detectable as it falls within the limits of the experimental precision (±30% for these weak NOEs).

The internucleotide NOEs are related to the base roll angle, the local pitch, and the helical twist angle, as well as the glycosidic torsion angle and puckers of the nucleotide units.

Table IV: Structural Changes in the Pribnow Box[a]

base	parameter	change (I → II)	value in state II	change (II → III)
T9	P	0	N(20)	0
	x	0	−35	0
	r	5	−13	4
T10	P	0	S	nd[b]
	x	0	−35	5
	r	11	3	0
A11	P	0	S(126)	N(54)
	x	10	−46	0
	r	10[c]	4	−10[c]
A12	P	0	S(126)	0
	x	6	−41	0
	r	7[d]	1	0
T9-A12′	θ_p	12	−12	3
	θ_r	−1	−7	2
	θ_t	6[c]	44	5
	h	1[c]	3.3	0.4
T10-A11′	θ_p	21	7	−10
	θ_r	1	−1	10
	θ_t	14	30	0
	h	0.4	3.6	0

[a] Changes in structural parameters were estimated from the data in Table II according to the text. The reference state is state II, for which the values of the parameters are given in the central column. The maximum possible changes in these values, consistent with the data for the transitions from the reference state to the other two states are given in the neighboring columns. The changes assume no covariance. P is the pseudorotation phase angle, $S(N)$ is the "south" ("north") conformation [i.e., C2′-endo-(C3′-endo)], x is the glycosidic torsion angle, r is the individual base pair roll, h is the local pitch, θ_t is the helical twist, θ_p is the propeller twist, and θ_r is the interbase pair roll angle. The last is defined as the angle between the mean planes of successive base pairs, positive opening toward the minor groove. θ_p and θ_r are calculated from the individual roll angles r. [b] nd, not determined. [c] These variations do not account for the changes in the NOEs between the sugar and base protons but do account for the changes in distance between the H2's of A11 and A12. [d] These variations are not compatible with the apparent A11–A12 H2 distance but imply changes in other parameters to compensate for the distance mismatch. See text.

It was not possible to determine the structures of states I and III, because it is necessary to obtain accurate NOEs for the whole sequence at each temperature to sort out the problem of overlap, which changes as the temperature is changed. However, simulations of the changes of the NOEs allow us to estimate the upper bounds on changes in structural parameters consistent with the observed NOEs, assuming no covariance. The simulations were performed by starting with state II, which we determined in the preceding article, and varying each parameter in turn. The results of the calculations are given in Table IV. Some maximum variations are intrinsically unlikely, such as the change of 1 Å in the pitch of A11–A12 or the 14° increase in the helical twist of T10–A11. Other changes support the observed intranucleotide NOE changes but are inconsistent with the estimated distances between the H2's of A11 and A12 (see above).

It is likely that more than one angle or pitch changes at the same time during the conformational transitions. Indeed, inspection of molecular models indicates that the structure of the nucleotide units and their relative orientations change in a compensating manner. For example, changes in the glycosidic torsion angle are compensated by base roll, whereas a change in the sugar pucker modifies the orientation of the base with respect to the plane of the sugar.

Observation of the data in Table IV lead us to propose a tentative model for the conformational changes. From state I to state II, a roll of the A11 base compensates for the change in the glycosidic torsion angle. At the same time, this would bring the H2's of A11 and A12 closer together and change the propeller twist of the A11–T10′ base pair (cf. Table IV).

In this transition, there is a trend for both central AT base pairs to flatten (the propeller twist becomes smaller). In the transition from state II to state III, the major conformational change is in the puckers of A11, accompanied by increases in the helical twist and local pitch. This results in an increase in the distance between the H2's of A1 and A12, corresponding to the NOE observation (see above). The amplitudes of these structural variations cannot be determined. Only the maximum amplitudes, assuming no covariance, are given in Table IV.

Potential Biological Relevance of Conformational Changes: A Modified Reaction Scheme for the Initiation of Transcription. The temperature-dependent conformational transitions we have observed are localized to the sequence TAA of the Pribnow box in the trp operator-promoter. We observed no structural changes elsewhere in the sequence, including the similar trinucleotides TAC and TAG. The latter triplet, like TAA, is found at the center of symmetry of a palindrome (Lefèvre et al., 1985b). TAA is an important feature of the Pribnow box sequence. From studies of mutant promoters, Hawley and McClure (1983) concluded that substitutions in the Pribnow box are up mutations if they tend to restore the consensus sequence and are down mutations if they destroy it. For example, the lac P promoter (TATAGT) is relatively weak (isomerization limited) but becomes a strong promoter when the G is replaced by A, giving the lac UV5 promoter (Hawley & McClure, 1983).

On the other hand, it is known that the initiation of transcription has a steep temperature dependence with a midpoint temperature in the range 15–25 °C, depending on the promoter sequence (Chamberlin, 1974; Richardson, 1975; Dausse et al., 1976; Suzucki et al., 1976). The thermodynamic parameters for binding RNA polymerase and the subsequent isomerization step (see Scheme I) have been obtained from studies of abortive initiation as a function of temperature (Bertrand-Burgraff et al., 1983; Buc & McClure, 1985). Using this technique, Buc and McClure (1985) have shown that another step should be included in the reaction scheme for initiation from the lac UV5 promoter. They proposed Scheme II, where an additional isomerization is included between the closed and open complexes. The assumption of the model is that the intermediate state, RPi, is populated at low temperatures and rapidly isomerizes to the open complex, RPo, at physiological temperature. The existence of RPi has also been suggested for the phage promoters A1 of phage T7 (Kadesh et al., 1982) and Pr of phage 1 (Roe et al., 1984) on the basis of different types of observations.

Scheme II

$$R + P \leftrightarrow RPc \leftrightarrow RPi \leftrightarrow RPo \rightarrow \text{transcription}$$

A direct comparison of the temperature of the midtransitions (t_m) we have observed in the trp promoter and the t_m of the activity of the RNA polymerase–promoter complex cannot be made, as there is no guarantee that the enzyme does not change the t_m of the transitions. Our observations on the trp promoter, and the importance of the sequence TAA in the Pribnow box (Lefèvre et al., 1985b), lead us to propose a new scheme (Scheme III) for the initiation of transcription derived from the already proposed ones and explicitly taking into account isomerizations in the free promoter, where PI, PII, and PIII are the three states described above and R denotes RNA polymerase haloenzyme. The arabic numerals refer to equilibrium constants and rate constants for the several possible transitions. We assume that PI, PII, and PIII are in rapid equilibrium among themselves [k(transition) $\approx$ 200 s^{-1}, see above] and with the states RPIc, RPIIc and RPIIIc. We further assume that only state RPIIIo is transcriptionally active, though in principle RIIi could also be active. The transitions denoted 2 are slow, and further, the states RPIi, RPIIi, and RPIIIo are stable, i.e., $k_2 \gg k_{-2}$.

Scheme III

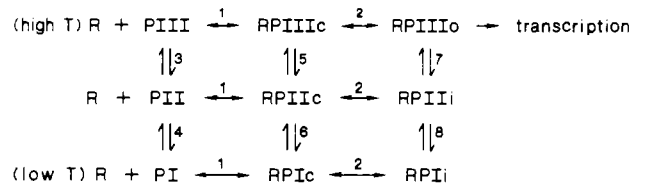

The RNA polymerase is likely to induce structural changes in the DNA, as the complex isomerizes toward an open complex, competent for initiating the transcription. Studies on the complex between the operator and the Trp repressor have indeed demonstrated the flexibility of the oligonucleotide (Lane et al., 1987c). However, the data do not give any information on the structure of the open-state complex. The model implies that different preexisting structures of the DNA will lead to different structures in the complex and will require different amounts of energy to be transformed into the competent open complex. For example, the energy required to transform the structure of the DNA from state I to the open state in the complex is probably too high and cannot be provided by the interaction between the DNA and the polymerase.

This model can account for the findings of Buc and McClure (1985). At temperatures lower than about 15 °C, the complex accumulates in RPIi. The rate constants for the transitions to states II and III being very low, the population in the active form is likely to be negligible and the transcription undetectable. The kinetics of formation of the active complex RPIIIo, if detectable, is very complicated due to the number of steps that the process involves. At intermediate temperature (between 15 and 30 °C), the reaction scheme becomes identical to Scheme II (Buc & McClure, 1985), which includes the intermediate complex RPi stabilized at low temperature (19 °C):

$$R + PII \overset{1}{\leftrightarrow} RPIIc \overset{2}{\leftrightarrow} RPIIi \overset{7}{\leftrightarrow} RPIIIo \rightarrow \text{transcription}$$

The kinetics of formation of RPIIIo should contain two exponentials, due to transitions 2 and 7. At high temperature (over 30 °C), where state III is mainly populated, the intermediate states are bypassed and the initiation of the transcription is then adequately described by the classical two-step model indicated in Scheme I. At this temperature, the kinetics for the appearence of RPIIIo contains only one exponential. Indeed, in the studies of the lac UV5 (Buc & McClure, 1985), the intermediate step was not observed above 29 °C.

The relative magnitude of some rate constants can be estimated from the results obtained on the lac UV5 (Buc & McClure, 1985) and the λ Pr promoters (Roe et al., 1984). In these studies, the dissociation rate constant of the open complex is smaller at high than at low temperature. This leads to a negative apparent activation energy and indicates that more than one step is involved in the process. In our model, this can be interpreted as a ranking of the k_{-2} rate constants, from high in state I to small in state III, so that the open complex RPIIIo is more stable than the pre open complexes RPni. The fact that the initiation of the transcription from the lac UV5 starts without a lag when the complex is brought back from 19 to 30 °C (Buc & McClure, 1985) indicates that at this latter temperature isomerization between RPIIi and

RPIIIo is faster than between RPIIIc and RPIIIo [$k_3 > k_2$-(III)].

Summary and Conclusions

We have observed temperature-dependent changes in the conformation of the Pribnow box of the trp promoter. The changes can be analyzed in terms of a three-state model (I, II, III). Only the two symmetric A11-T10′ base pairs are affected in both transitions. In the first transition, these base pairs flatten, whereas in the second the sugar pucker of A11 approaches C3′-endo. This is accompanied by an increase in the twist angle and local pitch for the step A11-A12. State I is the lowest energy conformation and is characterized by a large propeller twist for A11-T10′. According to Calladine (1982), base pair stacking is optimized for large base roll angles, which is often prevented by steric clashes in the minor groove for purine–pyrimidine steps. Thus, state I is expected to be a low-energy configuration for the sequence TAA. As the temperature is raised to about 25 °C, the propeller twist decreases to relieve steric clashes in the minor groove, contingent on movement of the bases. This leads to a decrease in stacking of A11 on A12. As the stacking energy is large (≈100 kcal/mol of base pair), one would expect a large enthalpy change for the transition I ↔ II; we observe an enthalpy change of 58 kcal/mol of cooperative unit (cf. Table I).

We note that Patel and co-workers (Patel et al., 1985) have also observed selective changes of proton chemical shifts as a function of temperature, on the consensus Pribnow box sequence CGATTATAATCG. These changes, attributed to a so-called premelting transition, were also localized to the trinucleotide TAA. The observed dependence of the chemical shifts of the H2's of the TAA sequence were consistent with a three- (or more) state transition. Interestingly, "premelting" was also observed in the sequence AATT (Patel et al., 1982) but not in TATA (Patel et al., 1985). These data support our proposal that the sequence TAA has special structural and dynamic properties.

Nonalternating AT sequences are known to have distinctive properties. For example, the electrophoretic mobilities of different sequences of AT bases pairs, of fixed composition and length, were consistent with kinks being present at the junctions between two or more adenines or thymines (e.g., TTAA) (Wilson et al., 1987). Crothers and co-workers have also demonstrated anomalous electrophoretic mobilities of DNA fragments associated with stretches of Adenines (Koo et al., 1986). Further, the influence of the sequence TTAA in transcription has been noted in other systems (Collins et al., 1985; Gelinas et al., 1985) and on stringent regulation of tyr T in *E. coli* (Lamond & Travers, 1985).

It is possible to correlate the rate of isomerization of the closed complex to the open complex (cf. Schemes I–III) with the presence or absence of TAA in the Pribnow box. In general, those promoters that contain TAA have a high isomerization rate constant (Lefèvre et al., 1985b). TAA appears to have conformational features that are essential for efficient promoters. We have proposed a new reaction scheme (Scheme III) for the initiation of transcription that takes into account the conformational flexibility of the Pribnow box.

Finally, there has been considerable interest in the relationship between the observed rates of exchange of the imino protons and biological function in control sites (Patel et al., 1985; Cheung et al., 1984). We have also studied in detail the exchange behavior of the imino protons of the trp operator-promoter (Lefèvre et al., 1985a) and have found significant sequence-dependent variations in the exchange rate constants. However, the rate constants for exchange of the imino protons of the AT base pairs in the Pribnow box are actually slower than those in other regions of the operator. Hence, we conclude that stability of the imino protons (and the relative populations of the exchange open state) does not correlate with the conformational transitions we have observed in the Pribnow box. This suggests that imino proton exchange rate constants do not report on the strength of promoters.

Registry No. RNA polymerase, 9014-24-8; CGTACTAGTTAACTAGTACG, 99637-95-3.

References

Arter, D. B., & Schmidt, P. G. (1976) *Nucleic Acids Res. 3*, 1437–1447.

Bertrand-Burgraff, E., Lefèvre, J.-F., & Daune, M. (1984) *Nucleic Acids Res. 12*, 1697–1706.

Bevington, P. R. (1969) *Data Reduction for the Physical Sciences*, Chapter 11, McGraw-Hill, New York.

Bothner-By, A. A., & Noggle, J. H. (1979) *J. Am. Chem. Soc. 101*, 5152–5160.

Buc, H., & McClure, W. R. (1985) *Biochemistry 24*, 2712–2723.

Calladine, C. R. (1982) *J. Mol. Biol. 161*, 343–352.

Chamberlin, M. J. (1974) *Annu. Rev. Biochem. 43*, 721–775.

Cheung, S., Arndt, K., & Lu, P. (1984) *Proc. Natl. Acad. Sci. U.S.A. 81*, 3665–3669.

Collins, F. S., Metherall, J. E., Yamakawa, M., Pan, J., Weissman, S. M., & Forger, B. G. (1985) *Nature (London) 313*, 325–326.

Dausse, J. P., Santenac, A., & Fromageot, P. (1976) *Eur. J. Biochem. 65*, 387–393.

Dickerson, R. E. (1983) *J. Mol. Biol. 160*, 419–441.

Gelinas, R., Endlich, B., Pfeiffer, C., Yagi, M., & Stamatoyanopoulos, G. (1985) *Nature (London) 313*, 323–324.

Hawley, D. K., & McClure, W. R. (1983) *Nucleic Acids Res. 11*, 2237–2255.

Jardetzky, O. (1982) *Biochim. Biophys. Acta 621*, 227–232.

Jardetzky, O., & Roberts, G. C. K. (1981) in *NMR in Molecular Biology*, Academic, New York.

Jernigan, R. L., Sarai, A., Ting, K.-L., & Nussinov, R. (1986) *J. Biomol. Struct. Dyn. 4*, 41–48.

Kadesch, T. R., Rosenberg, S., & Chamberlin, M. J. (1982) *J. Mol. Biol. 155*, 1–29.

Kearns, D. R. (1984) *CRC Crit. Rev. Biochem. 15*, 237–265.

Koo, H.-S., Wu, H.-M., & Crothers, D. M. (1986) *Nature (London) 320*, 501–506.

Lamond, A. I., & Travers, A. A. (1985) *Cell (Cambridge, Mass.) 41*, 6–8.

Lane, A. N., Lefèvre, J.-F., & Jardetzky, O. (1986a) *J. Magn. Reson. 66*, 201–218.

Lane, A. N., Lefèvre, J.-F., & Jardetzky, O. (1986b) *Biochim. Biophys. Acta 867*, 45–56.

Lane, A. N., Lefèvre, J.-F., & Jardetzky, O. (1986c) *Biochim. Biophys. Acta 909*, 58–70.

Lefèvre, J.-F., Land, A. N., & Jardetzky, O. (1985a) *J. Mol. Biol. 185*, 689–699.

Lefèvre, J.-F., Lane, A. N., & Jardetzky, O. (1985b) *FEBS Lett. 190*, 37–40.

Lefèvre, J.-F., Lane, A. N., & Jardetzky, O. (1987) *Biochemistry 26*, 5076–5090.

Patel, D. J., Kozlowsky, S. A., Marky, L. A., Broka, C., Rice, J. A., Itakura, K., & Breslauer, K. J. (1982) *Biochemistry 21*, 428–436.

Patel, D. J., Kozlowski, S. A., & Bhatt, R. (1983) *Proc. Natl. Acad. Sci. U.S.A. 80*, 3908–3912.

Patel, D. J., Koslowsky, S. A., Weiss, M., & Bhatt, R. (1985) *Biochemistry 24*, 936–944.

Richardson, J. P. (1975) *J. Mol. Biol. 91*, 477-487.
Roe, J. H., Burgess, R. R., & Record, T. R. (1984) *J. Mol. Biol. 174*, 495-521.
Rosenberg, M., & Court, D. (1979) *Annu. Rev. Genet. 13*, 319-353.
Sandström, J. (1982) *Dynamic NMR Spectroscopy*, Academic, London.
Siebenlist, U. (1979) *Nature (London) 279*, 651-652.
Suzycki, S. J., Suzycki, J. A., & Gussin, G. N. (1976) *Mol. Gen. Genet. 143*, 167-175.
Wagner, G., & Wüthrich, K. (1979) *J. Magn. Reson. 33*, 675-678.
Wilbur, D. W., DeFries, T., & Jonas, J. (1976) *J. Chem. Phys. 65*, 1783-1789.
Wilson, W. D., Zuo, E., Jones, R. L., Zon, G. L., & Baumstark, B. R. (1987) *Nucleic Acids Res. 15*, 105-118.

Dynamics of Repressor–Operator Recognition: The Tn*10*-Encoded Tetracycline Resistance Control†

Christoph Kleinschmidt,‡,§ Karlheinz Tovar,‖ Wolfgang Hillen,‖ and Dietmar Porschke*,§
Max-Planck-Institut für biophysikalische Chemie, 3400 Göttingen, FRG, and Institut für Mikrobiologie der Universität, 8520 Erlangen, FRG

Received April 1, 1987; Revised Manuscript Received October 14, 1987

ABSTRACT: Binding of the Tet repressor to nonspecific and specific DNA leads to quenching of the Tet fluorescence by ~22% and ~35%, respectively. This effect is used for a direct, quantitative characterization of the binding equilibria and dynamics involved in the recognition of the operator by its repressor. From the dependence of the nonspecific binding constant on the ion concentration, it is concluded that nonspecific binding is almost completely driven by the entropy change resulting from the release of three to four Na^+ ions from the double helix upon protein binding. Formation of the specific complex is driven by a higher entropy term resulting from the release of seven to eight Na^+ ions and in addition by a free energy term of −33 kJ/mol from nonelectrostatic interactions, which are attributed to the specific contacts. The dynamics of the repressor–operator recognition are resolved by stopped-flow measurements at various salt concentrations and for different DNA chain lengths into two separate steps. The first step follows a second-order mechanism and results in an intermediate complex associated with formation of about three to four electrostatic contacts between protein and DNA; apparently, this complex is equivalent to the nonspecific complex. The existence of an intermediate is also indicated by experiments in mixed Na^+–Mg^{2+} buffers, which can be described with high accuracy by competition of Mg^{2+} and protein. The intermediate complex is formed at a rate of 3×10^8 M^{-1} s^{-1} and is converted in the second reaction step to the specific complex with a rate constant of 6×10^4 s^{-1}, which is almost independent of the salt concentration. Our interpretation and the parameters obtained from our model are confirmed by competition of nonspecific DNA with operator DNA for repressor binding. The observed maximal rate constant of 3×10^8 M^{-1} s^{-1} is very close to theoretical predictions for the association without a sliding mechanism. The very small dependence of the observed rate constants on the chain length shows that the Tet repressor is not able to slide over any substantial distance even at low salt concentrations. The question of a potential contribution from sliding under our experimental conditions is critically discussed. The absence of sliding in the case of the Tet repressor under physiological conditions is compared with the high sliding efficiency of the *lac* repressor and is discussed with respect to possible molecular mechanisms of sliding in relation to biological function.

The recognition of DNA operators by their repressors is a key process in the regulation of gene activity and is well-known for its unusually high specificity. The *lac* repressor–operator system has been the main object for investigations of the specificity and dynamics of this reaction. As first demonstrated by Riggs et al. (1970a,b), the *lac* repressor not only shows a high degree of specificity but also has an unusually high rate of reaction, which appeared to be at first glance beyond the physical limits of diffusion-controlled reactions. A quantitative theoretical analysis (Adam & Delbrück, 1968; Richter & Eigen, 1974; Berg & Blomberg, 1976, 1977, 1978; Schranner & Richter, 1978; Berg et al., 1981) revealed that the high rate is due to an increase of the operator target size resulting from binding of the repressor to nonspecific DNA and sliding of the protein along the nonspecific sites. This effect leads to a reduction of the diffusion dimension from three to one and thus to a considerable increase of the association rate.

The rate parameters of the *lac* system had to be measured by the filter binding technique, which is rather indirect and subject to systematic errors. Because of the general importance of the repressor–operator reactions, it should be useful to study this type of reaction more directly, for example, by some spectroscopic technique. Thus, an initial observation of fluorescence quenching upon binding of the Tet repressor to DNA served as a basis for a systematic investigation of the specific and nonspecific binding reactions of this protein to DNA. The Tn*10*-encoded Tet repressor regulates the expression of tetracycline resistance in gram-negative bacteria

† This work was presented to the Technische Universität Braunschweig by C.K. in partial fulfillment of the requirements for the Ph.D. degree. W.H. was supported by grants from the Deutsche Forschungsgemeinschaft and the Fonds der chemischen Industrie.
‡ Present address: Max-Planck-Institut für Ernährungsphysiologie, 4600 Dortmund 1, FRG.
§ Max-Planck-Institut für biophysikalische Chemie.
‖ Institut für Mikrobiologie der Universität.

0006-2960/88/0427-1094$01.50/0